


An Observer Design Method Using Ultra-Local Model for Autonomous Vehicles

Daniel Fenyes¹ ^a, Tamas Hegedus¹, Vu Van Tan² and Peter Gaspar^{1,3}

¹*Institute for Computer Science and Control (SZTAKI), Eötvös Loránd Research Network (ELKH),
Kende u. 13-17, H-1111 Budapest, Hungary*

²*Department of Automotive Mechanical Engineering, Faculty of Mechanical Engineering,
University of Transport and Communications, 3 Cau Giay Street, 100000 Hanoi, Vietnam*

³*Department of Control for Transportation and Vehicle Systems, Budapest University of Technology and Economics,
Stoczek u. 2, H-1111 Budapest, Hungary*

Keywords: Observer, Model-Free Control, Ultra-Local Model, Lateral Velocity, Autonomous Vehicles.

Abstract: The paper presents a novel observer design algorithm for autonomous vehicles. The technique is based on the combination of a classical linear observer and the ultra-local model. The linear observer is easy to design and it requires only a linear model of the considered system. However, it performs poorly when the linear system cannot cover the system's dynamics due to nonlinearities or unmodelled dynamics. The ultra-local model aims to compensate for the nonlinear effects and improve the overall performances of the observer. The proposed method is applied to a vehicle-oriented estimation problem: lateral velocity. The operation and the effectiveness of the presented algorithm is demonstrated through several test scenarios in CarSim and also using real-test measurements.

1 INTRODUCTION AND MOTIVATION

The biggest challenges of the automotive industry are related to the development of highly automated, autonomous vehicles. Safe and reliable operation in every possible traffic situation is a prerequisite for the widespread of fully autonomous vehicles. The algorithm, which is responsible for vehicle control, contains several layers such as sensing, decision-making, and trajectory tracking. To guarantee the stable motion of the vehicle, the control systems require the continuous measurement of several states of the car such as velocities, angular velocities, and positions. Some of these signals can be well-measured using conventional onboard systems e.g. the angular velocities. However, other states are not directly measurable, e.g. lateral velocity. The estimation of the lateral velocity of the vehicle is a common problem, for which several solutions have been developed in the past decades. These solutions can be divided into two main groups:


- Model-based algorithms, which rely on mathe-

tical formulation of the vehicle dynamics.

- Non-model-based algorithms, which do not require a model but need a lot of training data of the vehicle dynamics, e.g. machine learning-based solutions.

One of the most common approaches to estimate the lateral velocity of the vehicle is Kalman filtering method. This technique combines several measurements from different sensors such as GPS and IMU with a kinematic model of the vehicle, see (Chu et al., 2010). The original Kalman filter can solely handle linear models, which results in conservative solutions. However, the extended Kalman filter is able to deal with nonlinear models using linearization methods around operating points of the system, see (Huang et al., 2017). Although these solutions have already been successfully applied to the estimation problem, they have serious drawbacks. Since Kalman-filter-based methods rely on accurate GPS signals, signal loss, which may occur, significantly reduces their performance level.

Other model-based approaches use the classical observation technique such quadratic optimization method (LQ) or polytopic modeling framework (LPV). To apply these techniques the considered sys-

^a  <https://orcid.org/0000-0002-6143-5599>

tem must be observable, which means that certain states of the system must be measurable.

LQ approach requires a linear model of the system, which is convenient in terms of the design process. But in the case of highly nonlinear systems, they provide less accurate estimations. LPV framework allows integrating a set of linear models to cover the whole nonlinear dynamics of the considered system, see (Kang et al., 2018),(Breschi et al., 2020). The advantages of the model-based methods include that they can provide theoretical guarantees. However, the efficiency and accuracy of these methods are significantly influenced by the modeling process and the accuracy of the yielded mathematical model. In addition, the effects of changing parameters must be taken into account to avoid performance degradation.

The second group of methods consists of solutions, which do not require a nominal model of the system, such as machine learning-based, and data-based approaches. In (Du et al., 2010) a neural network-based solution is presented for estimating the side-slip of the vehicle. Pace regression can also be used to determine the side-slip angle as proposed in (Fenyés et al., 2018). The advantage of these solutions is that the lack of the modeling process makes the design process easier, and also the nonlinear and uncertain effects can be handled more efficiently. However, these methods cannot provide stability guarantees, which are essential for safety-critical applications. There are other solutions, which aim to combine the classical and non-model-based approaches to eliminate their individual drawbacks. For example, in (Zhang et al., 2021) a method is proposed, which uses a Kalman filter and a neural network to compensate the effect of the possible GPS signal loss.

During the last decade, a new tool came up to efficiently solve modeling-related problems, called the ultra-local model-based approach (Fliess and Join, 2013). The motivation behind the original structure is to approximate the system in the given operating point. This means that the nonlinearities and uncertainties can be handled using the ultra-local model. However, the original concept has been proposed for a control system, and several works have been published in the field of observer design. In (Al Younes et al., 2015) a nonlinear observer method is proposed for aerial vehicles using the combination of the ultra-local model-based technique and a Thau observer design.

This paper aims to combine a linear observer design method for lateral velocity estimation with the results of the ultra-local model-based approach using real test datasets. The original structure is modified to take into account a priori knowledge of the system.

The modified structure is called the error-based ultra-local model (Hegedűs et al., 2022). Then, the whole design process is carried out for a vehicle model with a nominal parameter set. The advantage of the combined solution is that by using the ultra-local model-based part of the algorithm, the differences between the nominal model and the real system can be handled effectively. The proposed algorithm is tested on real measurement data with different test scenarios. The test scenarios have been carried out on ZalaZone proving ground using a Lexus RH450 test vehicle.

The paper is structured as follows: Section 2 presents the error-based ultra-local model and gives a short introduction to LQ observer design, then details the combined design approach. In section 3, the vehicle-oriented example is presented including the main steps. The effectiveness of the proposed algorithm is demonstrated in the vehicle simulation software, CarSim and using real test measurements in Section 4. Finally, the conclusion of the paper is summarized in Section 5.

2 OBSERVER DESIGN USING ULTRA-LOCAL MODEL

2.1 Error-Based Ultra-Local Model

The core idea of the error-based ultra-local model is to create two ultra-local models: First one is computed from the measured signals, second one is derived from reference signals. Then, the error-based ultra-local model (Δ_{nom}) is calculated as the deviation of two ultra-local models, see (Fenyés et al., 2022):

$$y^{(v)} = F + \alpha u \quad (1a)$$

$$y_{ref}^{(v)} = F_{nom} + \alpha u_{nom,ref} \quad (1b)$$

$$\underbrace{y^{(v)} - y_{ref}^{(v)}}_{e^{(v)}} = \underbrace{F - F_{nom}}_{\Delta_{nom}} + \underbrace{\alpha u - \alpha u_{nom,ref}}_{\alpha \tilde{u}} \quad (1c)$$

$$e^{(v)} = \Delta_{nom} + \alpha \tilde{u} \quad (1d)$$

where F is the ultra local model, u control signal, y measured output, v order of derivative, α denotes a free tuning parameter, y_{ref} is the reference output signal, $u_{nom,ref}$ denotes the referene control input The reference signal y_{ref} and the corresponding reference input signal, $u_{nom,ref}$.

Finally, the additional control input (\tilde{u}), which compensates the unmodelled dynamics of the system, can be computed as:

$$\tilde{u} = \frac{-\Delta_{nom,est}}{\alpha}, \quad (2)$$

2.2 Discrete Linear Quadratic Observer

Linear Quadratic Observer design is based on a discrete state-space representation of the considered system, which can be written, in general form, as:

$$x(k+1) = \Phi x(k) + \Gamma u(k) \quad (3a)$$

$$y(k) = c^T x(k) \quad (3b)$$

where Φ , Γ , c^T are state matrices, x is the state-vector, y is the output of the system, u is the control input while k denotes the time step. The estimated state-vector is computed as:

$$\hat{x}(k+1) = \Phi \hat{x}(k) + L(c^T x(k) - c^T \hat{x}(k)) \quad (4)$$

The goal of the observer design to minimize the error between the estimated states \hat{x} and the real states x :

$$e = x - \hat{x}, \quad |e| \rightarrow \min! \quad (5)$$

The error system can be written as (Kang and Kim, 2020):

$$e(k+1) = \Phi e(k) - L(c^T x(k) - c^T \hat{x}(k)) = \quad (6)$$

$$= (\Phi - Lc^T)e(k) \quad (7)$$

where L is the gain-vector, which contains the optimized gains for the observer.

This gain-vector can be computed by minimizing the following cost function:

$$J = \frac{1}{2} \sum_{i=1}^{\infty} (z_1^T(i) Q z_1(i) + z_2^T(i) R z_2(i)) \quad (8)$$

where $z_1 = x - \hat{x}$ is the performance, which minimizes the error between the real and estimated states, and $z_2 = L(y - \hat{y})$ is the control signal for correcting the estimated states while Q and R are weighting matrices. The optimal gain vector (L) can be computed by the discrete time algebraic Riccati equation, which can be formed as:

$$\Phi P + P \Phi^T - P c^T R^{-1} c P + Q = 0 \quad (9)$$

$$L^T = P c^T R^{-1} \quad (10)$$

where $P > 0$.

3 VEHICLE-ORIENTED APPLICATION

In the followings, the proposed observer design is presented for a vehicle-oriented estimation problem. The observer design consists of the following main steps:

1. The determination of the nominal model.
2. Selection of the required derivative order (v).

3. Computation of the nominal reference signals ($u_{nom,ref}, y_{ref}^v$)
4. Tuning of the parameter α .
5. Design of LQ observer based on the nominal model.
6. Finally, the estimated states can be computed as: $\hat{x}(k+1) = \Phi \hat{x}(k) + \Gamma(u(k) - \Delta(k)) + L(y(k) - \hat{y}(k))$

The structure of the observer algorithm is illustrated in Figure 1.

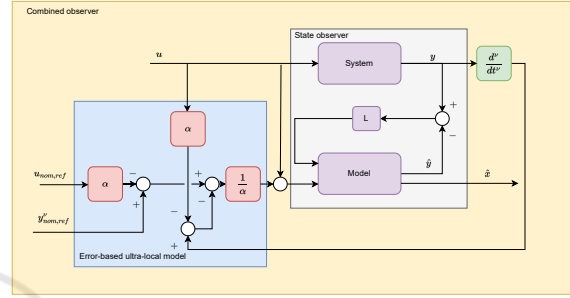


Figure 1: The structure of the proposed observer.

3.1 Determination of the Nominal Model

In this paper, the one-track bicycle model is used during the modeling phase of the lateral vehicle dynamics (Rajamani, 2005). The basic idea behind this model is that the front and rear wheels are replaced by one wheel each placed on the longitudinal axis of symmetry of the vehicle. The state-space representation of the model is given as:

$$\begin{bmatrix} \dot{y} \\ \dot{\Psi} \end{bmatrix} = \underbrace{\begin{bmatrix} -\frac{C_f + C_r}{mv_x} & \frac{C_f l_f - C_r l_r}{mv_x} - v_x \\ -\frac{C_f l_f - C_r l_r}{I_z v_x} & -\frac{C_f l_f^2 + C_r l_r^2}{I_z v_x} \end{bmatrix}}_{A_v} \begin{bmatrix} \dot{y} \\ \dot{\Psi} \end{bmatrix} + \underbrace{\begin{bmatrix} \frac{C_f}{m} \\ \frac{C_f l_f}{I_z} \end{bmatrix}}_{B_v} \delta \quad (11)$$

with $c_v^T = [0 \quad 1]$.

$\dot{\Psi}$ denotes the yaw-rate and I_z is the yaw-inertia of the vehicle. Moreover, C_i gives the cornering stiffness of the tires of the front and rear axes and β is the side-slip angle. Moreover, l_i gives distance from the axes to CoG (center of gravity) and v_x is the actual longitudinal velocity. The lateral position of the vehicle is given by y , whilst δ is the road wheel angle.

Finally, the continuous state-space representation transformed into a discrete one:

$$x_v(k+1) = \Phi_v x_v(k) + \Gamma_v u_v(k), \quad (12a)$$

$$y_v(k) = c_v^T x_v(k), \quad (12b)$$

3.2 Selection of Derivative Order and Computation of the Reference Signal

The goal of the observer design is to estimate the lateral velocity (v_y). Since the first derivative of the lateral velocity is the lateral acceleration, which is a directly measurable signal, ν is set to $\nu = 1$. Note that the measured lateral acceleration (a_y) has an additional component therefore it is computed as $\dot{v}_y = a_y - v_x\dot{\psi}$. The reference signals ($u_{nom,ref}, y_{ref}^v$) can be computed using a model predictive approach as detailed in (Fényes et al., 2022). Note that during the simulation/measurements, the vehicle is controlled by a simple PD controller. PD controller does not use the lateral velocity (v_y), therefore it does not interfere with the proposed observer method.

3.3 Tuning the Parameter α

In the literature, there is no elaborate method to determine the optimal value of α . The determination of the tuning value is solved using an iterative algorithm. As pointed out by (Polack et al., 2019), when $\alpha \rightarrow \infty$, the effect of the ultra-local model decreases and, in contrast, when $\alpha \rightarrow 0$, the ultra-local model becomes the major factor of the system. The computational process is based on a previously saved dataset, which contains the estimated \hat{v}_y and also the accurate value of the lateral velocity. In order to reach high-level performance not a constant α is used but it depends on the longitudinal velocity v_x , which is highly correlated to the nonlinear behavior of the vehicle. Therefore, the measured dataset Ω is sorted into subsets. Let $\mathcal{A}_i \in \mathbb{R}^{n \times 5}$, $\mathcal{A}_i = \{v_{y,i}, v_{y,i}, \dot{\psi}_i, \delta_i, a_{y,i}\}$ denote a measurement set, which includes the measured signals at a specific time step. The whole dataset consists of these measurement sets: $\mathcal{A}_i \in \Omega \quad \forall i \in \mathbb{N}^+$. Then, the dataset is divided into subsets $\{\omega_1, \omega_2 \dots \omega_n\} \subseteq \Omega$. A subset is determined by a specific range of longitudinal velocity $\mathcal{A}_i \in \omega_j \{v_{x,i} | v_{x,min,j} < v_{x,i} < v_{x,max,j}\}$ where $v_{x,min,j}$ and $v_{x,max,j}$ are the lower and upper bounds of j^{th} subset.

The following optimization process must be performed for each subset to get a set of $\alpha(v_x)$:

$$\min_{\alpha_j} \sum_{i=1}^n (v_{y,i} - \hat{v}_{y,i})^2, \quad v_{y,i} \in \omega_j \quad (13)$$

where j is the index of the subsets and n is the number of elements in j^{th} subset. $\hat{v}_{y,i}$ is computed from the elements of \mathcal{A}_i .

The main steps of the iterative algorithm, which must be performed for each subset, are the following:

1. Design a nominal observer using the nominal model.
2. Set the value of α to a high value.
3. Using the nominal observer and the actual value of α , evaluate the algorithm for a predefined test scenario.
4. Compute the value of the error between the reference value and the output of the system e_n , where n denotes the n^{th} iteration step.
5. If $e_n \geq e_{n-1}$ or $n > N_{max}$, quit the iteration.
6. Decrease the value of α then jump to Step 3.

3.4 LQ Observer Design

The goal of the observer design to minimize the error between the estimated and the measured lateral velocities:

$$e = x - \hat{x}, \quad |e| \rightarrow \min! \quad (14)$$

This performance can be guaranteed by appropriately chosen weighting matrices. In case of lateral velocity estimation, the matrices are chosen to $Q = \text{diag}(1000, 10)$, $R = 1$.

4 VALIDATION OF THE ALGORITHM

In this section, simulation results are presented to show the efficiency and the operation of the proposed observer design approach. Moreover, at the end of this section, an additional example is presented based on a real measurement dataset. The whole algorithm has been implemented in MATLAB/Simulink and CarSim environment. During the simulations, a B-class passenger car is used, whose nominal parameter can be found in Table 1. Note that, the longitudinal velocity (v_x) is fixed to $v_x = 10m/s$ during the linear quadratic observer design.

Table 1: Parameters of the test vehicle.

m	1223 (kg)
l_f, l_r	1.083, 1.257 (m)
I_z	2330 (kgm^2)
C_f, C_r	123000, 110000 (N/rad)
v_x	10 (m/s)

In the followings, three simulations example are presented. In the first simulation, the vehicle is driven along a track with varying longitudinal velocity and two observer algorithms are used to estimate the lateral velocity: the proposed method and the nominal

LQ observer. In the second simulation, the friction coefficient of the tire-ground contact is decreased to $\mu = 0.5$, which aims to show the operation of the proposed observer method under extraordinary circumstances. In the last simulation, the type of the vehicle is changed, which means that the nominal model significantly differs from the real vehicle.

4.1 Results of Tuning α

The presented tuning algorithm is performed on a set of previous simulation from the simulation software, CarSim. The test scenarios include lane change maneuvers with $v_x = \{1 - 120\}km/h$, and sinusoidal steering signals. The resulted α values for each subset can be found in Figure 2. It has a progressive part between $v_x = \{1 - 80\}km/h$ and it reaches a constant value around $v_x = 120km/h$.

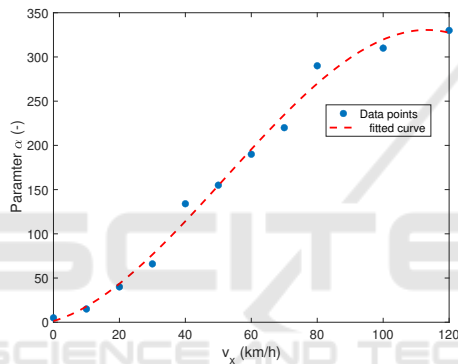


Figure 2: Parameter α .

4.2 Comparison of the Observers Under Standard Circumstances

In the first simulation, the vehicle is driven along F1 track of Hungary, shown in Figure 3. The track contains several sharp bends, where the lateral velocity can reach a high value. Furthermore, the longitudinal velocity of the vehicle varies as illustrated in Figure 4. The velocity profile consists of two main parts: the first one is the rapid changing part $t = \{0 - 200\}s$ and a slow changing part $t = \{200 - 400\}s$ in order to cover the whole operating range of the vehicle. Moreover, the measured signals ($a_y, \dot{\psi}$) are corrupted with white noises, whose variances: $\sigma_{a_y}^2 = 0.04$ and $\sigma_{\dot{\psi}}^2 = 0.01$.

Figure 5 shows the lateral acceleration of the vehicle during the test scenario. It can be seen, that maximum of a_y is around $8m/s^2$, which is close to the physical limit of the vehicle. In figure 6 similar phenomenon can be observed, the maximum of yaw-rate is about $0.6rad/s$. In summary, it can be concluded,

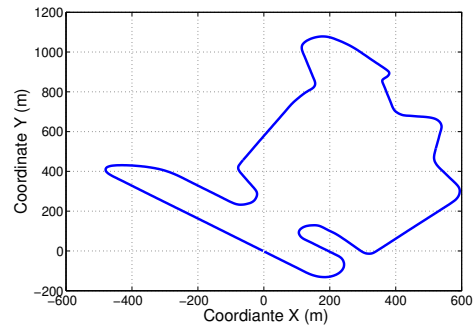


Figure 3: Test track.

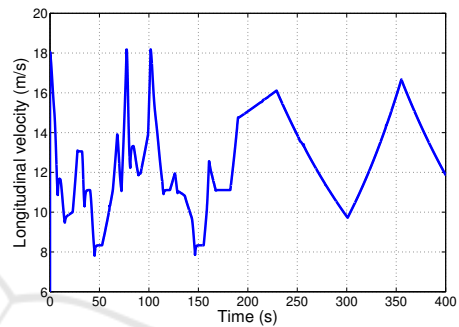


Figure 4: Longitudinal velocity of the vehicle.

that the simulations cover the whole operating range of the vehicle.

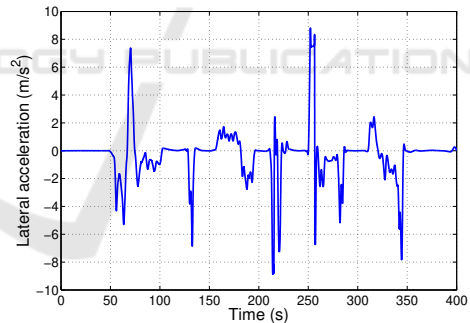


Figure 5: Lateral acceleration of the vehicle.

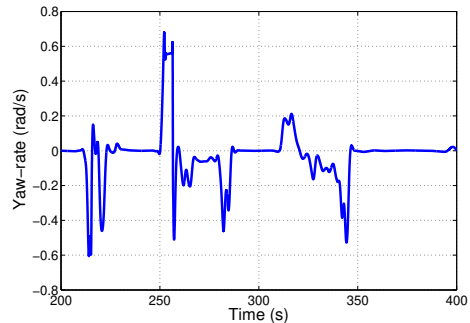


Figure 6: Yaw-rate of the vehicle.

The estimated and the measured lateral velocities are depicted in Figures 7,8. Note that, this signal is shown without the applied sensor noises. In the first section of the simulation, both observers provide good results, however in the second half, the nominal LQ observer has a significant error. At that section, the longitudinal velocity exceeds the nominal value ($v_x = 10m/s$) for a long period of time, therefore the LQ observer cannot provide good result. However, it can be seen, when the velocity close to the nominal value ($t = 300s$) the observer provides accurate results. In contrast, the combined observer algorithm estimate the lateral velocity in the whole simulation with low error.

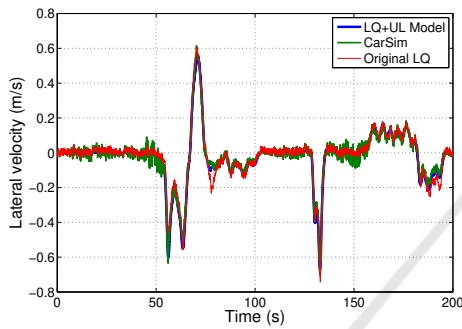


Figure 7: Estimated and measured lateral velocities $t = \{0 - 200\}s$.

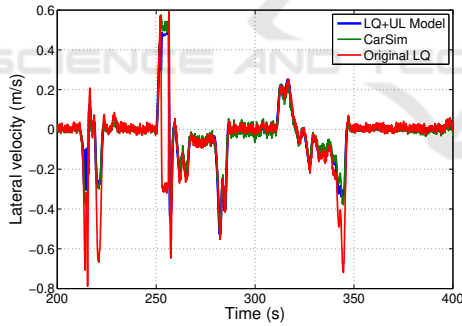


Figure 8: Estimated and measured lateral velocities $t = \{0 - 200\}s$.

The last figure demonstrates the control inputs of the observer. The blue line illustrates the computed error-based ultra-local model (Δ_{nom}) while the red line is the steering angle provided by the simulation software. In general, the ultra-local model has a higher amplitude, which aims to compensate for the unknown and unmodeled part of the system.

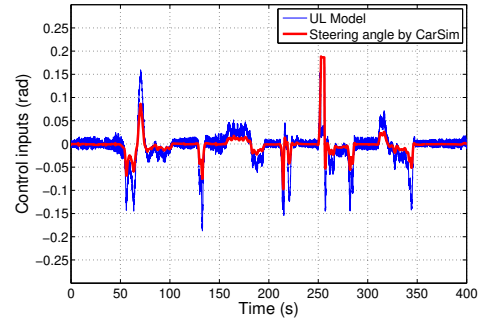


Figure 9: Inputs of the observers.

4.3 Simulation with Low Adhesion Coefficient

In the second simulation, the adhesion coefficient between the tire and ground changed to $\mu = 0.5$. This demonstrates a case when the vehicle travels on the snowy ground. Figure 10 shows the lateral acceleration during this test scenario. The maximum value of a_y decreases to $a_y = 4m/s^2$, which is caused by the low μ surface. It can also be seen, that the vehicle reaches that value several times during the simulation, which means that the vehicle loses its motion stability. The nominal, linear observer cannot cope with this motion as illustrated in Figures 11,12. In other cases, the observer still provides acceptable results. The combined observer, however, can deal with this nonlinear dynamics of the vehicle, and its result matches with the measured lateral velocity as shown in Figures 11,12.

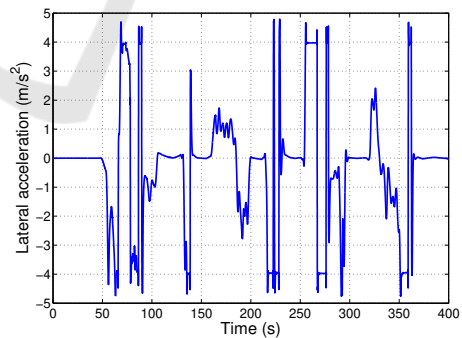


Figure 10: Lateral acceleration in case of low μ .

4.4 Simulation Using Different Vehicle Parameters

In the last test scenario, a case is investigated, when the designed observer is applied to a completely different vehicle. The goal of this simulation is to show the robustness of the proposed observer method. The selected vehicle is a D-class passenger car, whose pa-

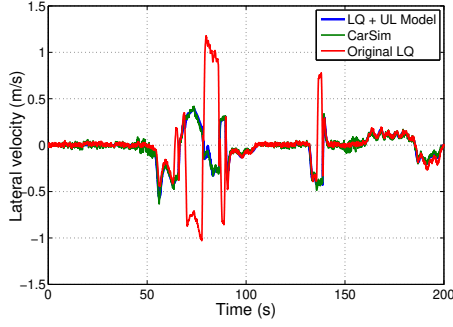
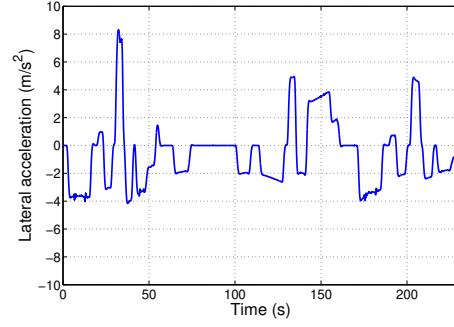

 Figure 11: Estimated and measured lateral velocities $t = \{0 - 200\}s$.


Figure 13: Lateral acceleration in case of D-class car.

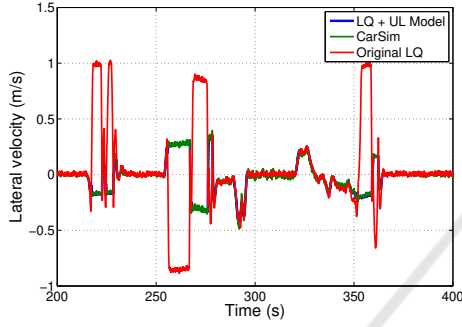
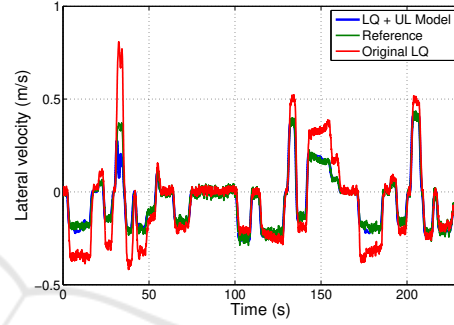

 Figure 12: Estimated and measured lateral velocities $t = \{200 - 400\}s$.


Figure 14: Estimated and measured lateral velocities in case of D-class car.

rameters can be found in Table 2. The track of the vehicle is also changed to Michigan Waterford race-track.

Table 2: Parameters of D-class car.

m	2013 (kg)
l_f, l_r	1.24, 1.68 (m)
I_z	4230 (kgm^2)
C_f, C_r	230000, 180000 (N/rad)
v_x	10 (m/s)

The lateral velocity of the vehicle is depicted in Figure 13. In this case, the maximum value of a_y is about $8m/s^2$, which indicates that the vehicle reaches its psychical limits in this scenario similarly to the previous test scenarios.

The estimated and the measured lateral velocities can be seen in Figure 14. As it can be seen, the nominal observer estimates the lateral velocity with a large error since the model parameters significantly differ from the real ones. However, the proposed observer still works well despite a short section between $t = \{30 - 35\}s$. Note that the tuning parameter α has also not been returned for this vehicle, which can be the reason behind this phenomenon.

4.5 Example Using Real-Test Measurements

To validate the performance of the proposed observer algorithm, a 2km long test scenario has been performed on the test ground using a Lexus RX450h test vehicle. CarSim model is used to compare the results of the observer and the measured data. This scenario includes several bends, varying longitudinal velocity with high acceleration and deceleration profile. Figure 15 illustrates the longitudinal velocity of the vehicle during the test. Its maximal value is about $25m/s$ while the lowest value is $5m/s$. Thus, the performance of the observer can be tested in a wide range of the vehicle dynamics. Figure 16 shows the measured and the estimated lateral velocities. As the figure illustrates, LQ-based observer provides poor results at low and high longitudinal velocities. Whilst, the proposed observer and CarSim's model covers the measured lateral velocity well. The maximum of the error is about $0.04m/s$ between $140 - 150s$. In other cases, the error is smaller than $0.02m/s$.

Figure 17 demonstrates the lateral acceleration during the test. The maximum of a_y is almost $6m/s^2$, which is high value for a SUV car. However, it does not influence the accuracy of the estimation.

Figure 18 shows the two input signals: steering angle and the output of the error-based ultra-local

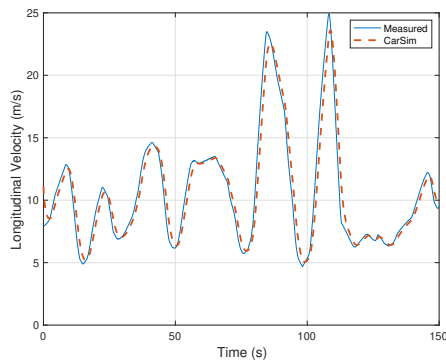


Figure 15: Longitudinal velocities of the vehicle.

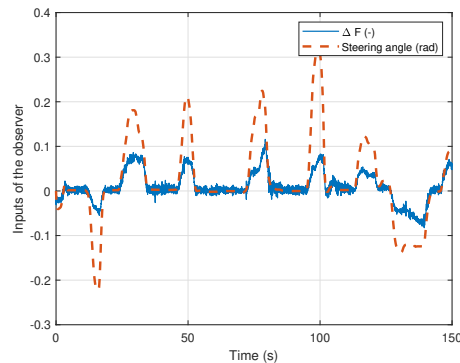


Figure 18: Control inputs.

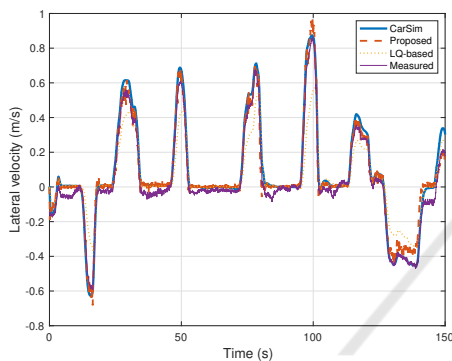


Figure 16: Lateral velocities of the vehicle.

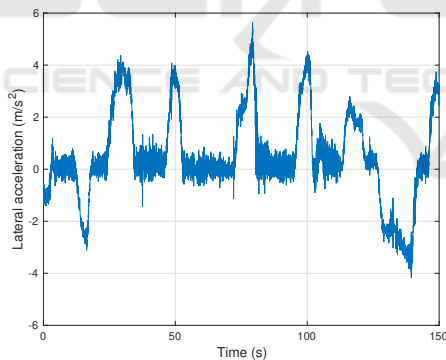


Figure 17: Lateral acceleration.

model. In this case, CarSim provides slightly worse results compared to the previous test. The maximal deviation appears at low longitudinal velocity for instance: 90 – 100s. The reason behind this phenomenon could be that CarSim’s dynamical model is fitted for higher longitudinal velocities. In the reasonable operating range, it fits well the measurements.

5 CONCLUSION AND FUTURE PLANS

In this paper, a novel combined observer design method has been proposed using the linear quadratic and the ultra-local model approaches. The LQ observer was designed on a nominal model, which was not expected to be accurate. The ultra-local model-based part was able to approximate the unmodeled dynamics of the system and to eliminate its effect, which resulted in a more accurate estimation of the observed state. The proposed observer design algorithm has been implemented to a vehicle-oriented estimation problem: lateral velocity. The effectiveness and the operation of the presented algorithm have been demonstrated through simulation examples using CarSim and a real test measurement. The future research directions include the investigation of co-design with the Model-Free Controller and the analysis of the closed-loop system.

ACKNOWLEDGEMENTS

The paper was funded by the National Research, Development and Innovation Office under OTKA Grant Agreement No. K 143599. The work of Daniel Fenyes was supported by the Janos Bolyai Research Scholarship of the Hungarian Academy of Sciences. The research was partially supported by the European Union within the framework of the National Laboratory for Autonomous Systems (RRF-2.3.1-21-2022-00002). The research was also supported by the National Research, Development and Innovation Office through the project "Cooperative emergency trajectory design for connected autonomous vehicles" (NK-FIH: 2019-2.1.12-TÉT_VN).

REFERENCES

- Al Younes, Y., Noura, H., Mufflehi, M., Rabhi, A., and El Hajjaji, A. (2015). Model-free observer for state estimation applied to a quadrotor. In *2015 International Conference on Unmanned Aircraft Systems (ICUAS)*, pages 1378–1384.
- Breschi, V., Formentin, S., Rallo, G., Corno, M., and Savaresi, S. M. (2020). Vehicle sideslip estimation via kernel-based lpv identification: Theory and experiments. *Automatica*, 122:109237.
- Chu, L., Shi, Y., Zhang, Y., Liu, H., and Xu, M. (2010). Vehicle lateral and longitudinal velocity estimation based on adaptive kalman filter. In *2010 3rd International Conference on Advanced Computer Theory and Engineering (ICACTE)*, volume 3, pages V3–325–V3–329.
- Du, X., Sun, H., Qian, K., Li, Y., and Lu, L. (2010). A prediction model for vehicle sideslip angle based on neural network. In *2010 2nd IEEE International Conference on Information and Financial Engineering*, pages 451–455.
- Fényes, D., Hegedűs, T., Németh, B., Szabo, Z., and Gáspár, P. (2022). Robust control design using ultra-local model-based approach for vehicle-oriented control problems. In *2022 European Control Conference (ECC)*, pages 1746–1751.
- Fényes, D., Hegedűs, T., Nemeth, B., Szabo, Z., and Gaspar, P. (2022). Combined lpv and ultra-local model-based control design approach for autonomous vehicles. In *2022 IEEE 61st Conference on Decision and Control (CDC)*, pages 3303–3308.
- Fényes, D., Nemeth, B., Asszonyi, M., and Gaspar, P. (2018). Side-slip angle estimation of autonomous road vehicles based on big data analysis. In *26th Mediterranean Conference on Control and Automation*, pages 849–854.
- Fliess, M. and Join, C. (2013). Model-free control. *International Journal of Control*, 86(12):2228–2252.
- Hegedűs, T., Fényes, D., Németh, B., Szabó, Z., and Gáspár, P. (2022). Design of model free control with tuning method on ultra-local model for lateral vehicle control purposes. pages 4101–4106.
- Huang, Y., Bao, C., Wu, J., and Ma, Y. (2017). Estimation of sideslip angle based on extended kalman filter. In *Journal of Electrical and Computer Engineering*.
- Kang, C. M. and Kim, W. (2020). Linear parameter varying observer for lane estimation using cylinder domain in vehicles. *IEEE Transactions on Intelligent Transportation Systems*, pages 1–10.
- Kang, C. M., Lee, S.-H., and Chung, C. C. (2018). Discrete-time lpv h_2 observer with nonlinear bounded varying parameter and its application to the vehicle state observer. *IEEE Transactions on Industrial Electronics*, 65(11):8768–8777.
- Polack, P., Delprat, S., and d'Ándrea Novel, B. (2019). Brake and velocity model-free control on an actual vehicle. *Control Engineering Practice*, 92:104072.
- Rajamani, R. (2005). *Vehicle dynamics and control*. Springer.
- Zhang, B., Zhao, W., Zou, S., Zhang, H., and Luan, Z. (2021). A reliable vehicle lateral velocity estimation methodology based on sbi-lstm during gps-outage. *IEEE Sensors Journal*, 21(14):15485–15495.